IAC-14,C4,P,64,x24415

Evaluations of Data Reduction Methods for Hybrid Rockets

Harunori Nagata
Faculty of Engineering, Hokkaido University, Japan, nagata@eng.hokudai.ac.jp

Yuji Saito
Graduate School of Engineering, Hokkaido University, Japan, yuji_space_hayabusa@yahoo.co.jp
Tatsuya Ishiyama
Graduate School of Engineering, Hokkaido University, Japan, wildprince_touch@frontier.hokudai.ac.jp
Yasuhiko Inaba
Graduate School of Engineering, Hokkaido University, Japan, inaba@frontier.hokudai.ac.jp
Masashi Wakita
Faculty of Engineering, Hokkaido University, Japan, m-wakita@eng.hokudai.ac.jp
Tsuyoshi Totani
Faculty of Engineering, Hokkaido University, Japan, tota@eng.hokudai.ac.jp

Accuracies and applicable ranges of five data reduction methods, RT-1 to RT-5, were evaluated experimentally, where a data reduction method is to obtain fuel consumption rate from measurable data such as chamber pressure and oxidizer flow rate. RT-1 determines the fuel consumption rate as a function of time from histories of the chamber pressure and the oxidizer flow rate, assuming a constant c^* during firing. Three of other methods obtain O/F (=ξ) by solving an equation between theoretical and experimental c^* values without assuming a constant c^*. RT-2 uses histories of chamber pressure and oxidizer flow rate, assuming a constant c^* efficiency. The third and fourth one (RT-3 and RT-4) eliminates the need for the assumption of a constant c^* efficiency by employing thrust history as additional input data. The difference between the two methods is that RT-3 assumes a constant nozzle discharge coefficient whereas RT-4 assumes a constant thrust deduction coefficient. From RT-2 to RT-4, a difficulty arises when multiple solutions of ξ exists in the equation between theoretical and experimental c^* values. RT-5 avoids this difficulty by merging two methods: RT-1 and RT-2. Because the c^* variation due to the ξ shift during a firing is not an uncommon feature in a hybrid rocket, the constant c^* assumption can cause error. The error in ξ increases with increasing the fluctuation range of ξ in a firing test. Experimental results show that ξ fluctuation of 10% can cause errors of around 6% in ξ. RT-2 can cause error due to the constant c^* efficiency assumption. Although the c^* efficiency does not change unless the flow field structure greatly changes, it still requires attention because only 3% of c^* efficiency fluctuation can cause up to 8% error in ξ. RT-5 can cause an error due to the use of ξ obtained by RT-1 for the function giving theoretical c^*. Although the error of RT-5 (=δ_5) is comparable to the error of RT-1 (=δ_1) in a certain ξ range, δ_5 is still less than δ_1. Accordingly, RT-5 can overcome the multiple solution problem and gives ξ more accurately than RT-1.

NOMENCLATURE

A_t = nozzle throat area
A_e = nozzle exit area
c^*_{ex} = experimental characteristic exhaust velocity obtained by Eq. (2)
$\bar{c}^*_{ex}$ = averaged experimental characteristic exhaust velocity obtained by Eq. (3)
c^*_{th} = theoretical characteristic exhaust velocity
$\dot{m}_f$ = instantaneous fuel mass flow rate (a function of time)
$\dot{m}_o$ = instantaneous oxidizer mass flow rate (a function of time)
$\dot{m}_p$ = instantaneous propellant mass flow rate (a function of time)
M_o = total oxidizer mass
M_f = total fuel mass
p_a = ambient pressure
p_e = isentropic one-dimensional pressure at nozzle exit (a function of time)
p_c = instantaneous combustion chamber pressure (a function of time)
t_b = burning duration
v_e = isentropic one-dimensional velocity at nozzle exit (a function of time)
ε_{ij} = mean relative error between RT-i and RT-j (i, j = 1, 2, …, 5) defined by Eq. (12)
η = c^* efficiency defined by Eq. (6)
λ_1 = nozzle discharge coefficient
λ_2 = thrust deduction coefficient
ω_ξ = fluctuation range of ξ defined by Eq. (11)
ω_η = fluctuation range of c^* efficiency defined by Eq. (13)

ξ = oxidizer to fuel ratio

$\bar{\xi}$ = mean oxidizer to fuel ratio defined in Eq. (11)

ξ_i = oxidizer to fuel ratio obtained by RT-i (i, j = 1, 2, …, 5)

I. INTRODUCTION

Because hybrid rockets have attracted attentions of many researchers due to their virtues such as safety, low cost, reduction of environmental burdens, and so on, there has been considerable research on it. In static firing tests of hybrid rockets, data reduction presents unique challenges comparing with other types of chemical rockets. In liquid rocket firings, a feed system supplies liquid propellants into a combustion chamber and propellant flow rates are directly-measurable. In solid rocket firings, the oxidizer to fuel ratio (ξ) is a known value and one can easily calculate the gasification rate of a solid propellant from chamber pressure and nozzle throat area, assuming a constant characteristic exhaust velocity (c^*) efficiency during a firing. A hybrid rocket employs a combination of solid and liquid propellants. Generally, the fuel is the solid side. Although the flow rate of the liquid oxidizer is directly-measurable, it is not for the solid fuel. Because c^* strongly depends on ξ, the direct calculation of the flow rate from chamber pressure and nozzle throat area like a solid rocket case is not possible.

Many traditional data reduction methods in hybrid rocket firings rely on endpoint averaging. Endpoint averaging uses the information of initial and final fuel shapes with the firing duration to determine the average fuel regression rate and the average fuel flow rate. A difficulty comes from the fact that both the regression rate and the fuel flow rate are neither constant during a firing nor linear functions of time. Many combustion experiments have been designed to use short firing durations to minimize this difficulty. However, errors associated with the ignition and shutdown transients can be significant in this case[1]. Another issue to be concerned is that the averaging technique is not unique due to the nonlinear nature of the fuel regression. Different averaging techniques can provide different regression rate laws for the same set of test data as Karabeyoglu et al. pointed out[2].

Some researchers have developed various reconstruction techniques to obtain fuel consumption rate from measurable data such as chamber pressure and oxidizer flow rate. To our knowledge, Osmon[3] made the earliest attempt. He developed a method of determining the fuel consumption rate as a function of time from histories of the chamber pressure and the oxidizer flow rate, assuming a constant c^* (characteristic exhaust velocity) efficiency. However, the theoretical c^* he used did not include the effect of chamber pressure. Also, he did not indicate how he could determine the averaged experimental c^*. The averaged experimental c^* necessary in this method is different from an experimental c^* widely used, and a complex iterative calculation is necessary to obtain this value[4]. George et al.[5] employed a similar approach but included the chamber pressure effect in the theoretical c^*. The authors[6] have also used this method. No specialized equipment is necessary in this method, but it requires a long computation time because a number of complex chemical equilibrium calculations are necessary in two stages of iterative calculations[4]. Wernimont and Heister[7] avoided this difficulty by assuming a constant c^* during firing. However, this assumption is unrealistic because the c^* variation due to the ξ shift during a firing is not an uncommon feature in hybrid rockets. Carmicino and Sorge[8] eliminated the need for the assumption of a constant c^* efficiency by employing a thrust history as an additional input data. They showed that the c^* efficiency does not change unless the flow field structure greatly changes. As a result, the assumption of a constant c^* efficiency is reasonable in many cases.

A main purpose of this research is to evaluate accuracies and applicable ranges of some data reduction methods experimentally. Five data reduction methods were applied to static firing tests with 10 kN and 500 N thrust class hybrid rocket motors. The first one (RT-1) is from Wernimont and Heister[7], which determines the fuel consumption rate as a function of time from histories of the chamber pressure and the oxidizer flow rate, assuming a constant c^* during firing. As noted before, this assumption is unrealistic because the c^* likely varies due to the ξ shift during firing in hybrid rockets. Three of other methods obtain ξ by solving an equation between theoretical and experimental c^* values without assuming a constant c^*. The second one (RT-2) is from George et al.[5], which uses histories of chamber pressure and oxidizer flow rate, assuming a constant c^* efficiency. The third and fourth one (RT-3 and RT-4) eliminates the need for the assumption of a constant c^* efficiency by employing thrust history as additional input data. The difference between the two methods is that RT-3 assumes a constant nozzle discharge coefficient whereas RT-4 assumes a constant thrust efficiency. The method of Carmicino and Sorge[8] corresponds to RT-3. From RT-2 to RT-4, a difficulty arises when multiple solutions of ξ exists in the equation between theoretical and experimental c^* values[4]. Three kinds of fuels (polyethylene, polystyrene, and PMMA) were examined with combinations of liquid oxygen (LOX), and one of them (PMMA) showed this difficulty in a certain ξ range. The fifth method, RT-5 avoids this difficulty by merging two methods: RT-1 and RT-2. Although RT-5 can avoid the multiple solution problem, it causes considerable error in certain conditions. Evaluating the accuracy and applicable range of RT-5 is another purpose of this research.

II. DATA REDUCTION METHOD

The following equations give instantaneous values of the total mass flux and the experimental characteristic exhaust velocity;

$$\dot{m}_p = \dot{m}_o + \dot{m}_f = \dot{m}_o\left(1+\frac{1}{\xi}\right) \tag{1}$$

$$c^*_{ex} = \frac{p_c A_t}{\dot{m}_p} = \frac{p_c A_t}{\dot{m}_o\left(1+\frac{1}{\xi}\right)} \tag{2}$$

In RT-1, we assume a constant c^*_{ex} being equal to $\bar{c}^*_{ex}$ given by the following equation;

$$\bar{c}^*_{ex} = \frac{\int_0^{t_b} p_c dt \cdot A_t}{M_o + M_f} \tag{3}$$

By substituting $\bar{c}^*_{ex}$ to c^*_{ex} in Eq. (2) and solve for ξ, the following equation gives ξ as a function of time;

$$\xi == \frac{\bar{c}^*_{ex}\dot{m}_o}{p_c A_t - \bar{c}^*_{ex}\dot{m}_o} \tag{4}$$

In RT-2, we assume that c^* is not a constant and varies with time. A theoretical calculation[9] provides a theoretical characteristic exhaust velocity as a function of ξ and the chamber pressure;

$$c^*_{th} = c^*_{th}(\xi, p_c) \tag{5}$$

By introducing the c^* efficiency η, we can obtain the following equation,

$$\eta c^*_{th}(\xi, p_c) = \frac{p_c A_t}{\dot{m}_o\left(1+\frac{1}{\xi}\right)} \tag{6}$$

in which we assume a constant c^* efficiency η during a firing. Unknown values in the above equation are η and ξ. By assuming a value for η, we can obtain ξ by solving the above equation. After obtaining ξ, the following equation provides the instantaneous value of the fuel flow rate;

$$\dot{m}_f = \frac{\dot{m}_o}{\xi} \tag{7}$$

The integral of the above equation gives the total fuel mass consumption during a firing;

$$M_f = \int_0^{t_b} \dot{m}_f dt = \int_0^{t_b} \frac{\dot{m}_o}{\xi} dt \tag{8}$$

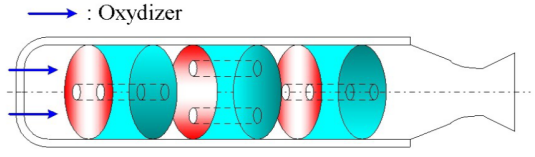

Fig. 1: Schematic view of a CAMUI type hybrid fuel grain.

An iterative calculation is necessary to adjust the value of η so that the calculated total fuel mass consumption agrees with the experimental result.

To remove the need for the constant c^* efficiency assumption, RT-3 and RT-4 employs thrust history as additional input data. RT-3 assume a constant nozzle discharge coefficient (=λ_1); the following equation gives thrust;

$$\begin{aligned} F &= \lambda_1 v_e\left(\dot{m}_o + \dot{m}_f\right) + \left(p_e - p_a\right)A_e \\ &= \lambda_1 v_e \dot{m}_o\left(1+\frac{1}{\xi}\right) + \left(p_e - p_a\right)A_e \end{aligned} \tag{9}$$

In equations (6) and (9), unknown values are η, ξ, and λ_1. By assuming a value for λ_1, we can obtain η and ξ by solving these two equations. The same iterative calculation as that of RT-2 follows to obtain λ_1. RT-4 is the same as RT-3 except that it assumes a constant thrust deduction coefficient and employs the following equation instead of Eq. (9);

$$\begin{aligned} F &= \lambda_2\left[v_e\left(\dot{m}_o + \dot{m}_f\right) + \left(p_e - p_a\right)A_e\right] \\ &= \lambda_2\left[v_e \dot{m}_o\left(1+\frac{1}{\xi}\right) + \left(p_e - p_a\right)A_e\right] \end{aligned} \tag{10}$$

Because RT-2, RT-3, and RT-4 calculates the fuel flow rate by solving Eq. (6), we encounter a difficulty when Eq. (6) has multiple solutions[4]. RT-5 avoids this difficulty by using ξ obtained by RT-1 in the left-hand side of Eq. (6). Except this, the procedure is the same as that of RT-2.

III. STATIC FIRING TESTS

Although test motors we employed in this research is those of CAMUI type[6], the present reconstruction techniques are applicable to all types of hybrid motors. The name CAMUI comes from an abbreviation of "cascaded multistage impinging-jet" representing the new fuel grain design Fig. 1 shows. By changing a conventional cylinder-shape solid fuel with a central port into multiple stages of cylinder blocks, end faces of all blocks burn concurrently. The grain design makes the combustion gas collide repeatedly with fuel surfaces, resulting in intense heat transfer to the fuel. We employed two test motors; 10 kN thrust class (Motor-A) and 1.2 kN

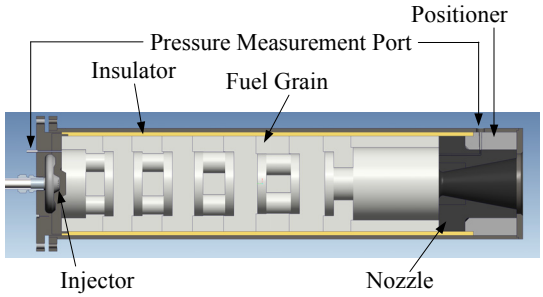

Fig. 2: Detail of test motors.

	Motor-A	Motor-B
Rated thrust	10 kN	1.2 kN
Nozzle		
Throat diameter	56 mm	13.5 mm
Exit diameter	123 mm	13.5 mm
Fuel	Polyethylene	PMMA
Fuel grain		
Diameter	200 mm	70 mm
Number of stages	9	3
Initial weight	25.4 kg	683 g

Table 1: Specifications of test motors.

thrust class (Motor-B) motors. Figure 2 shows the detail of the test motors. Each of them consists of an injector, a combustion chamber, and a nozzle. Liquid oxygen (LOX) flows into the combustion chamber through a pair of injectors. A fuel grain consists of several cylindrical fuel blocks and fuel spacers made of polyethylene or poly-methyl-methacrylate (PMMA). Each fuel block has two axial ports at axially opposite locations with each other. Adjoining injectors or ports are in 90-degree staggered orientation with each other to make the combustion gas or oxidizer streams collide repeatedly with fuel surfaces. Table 1 shows specifications of the two test motors.

Figure 3 shows the outline of the experimental apparatus. It mainly consists of a pressurization device using helium, a LOX reservoir, and a test motor. Heat insulating materials wraps LOX lines. These lines were cooled enough before each test. As a noteworthy feature in the LOX feeding system, there is no valve in the liquid oxygen line. Before starting liquid oxygen feeding, evaporating oxygen gas (GOX) outflows from the reservoir to the motor through the 3-way valve. This evacuation serves two purposes; one is to avoid self-pressurization of the liquid oxygen and the other is to help ignition of an igniter fuel on the upstream end face of the uppermost fuel block. A nichrome wire ignites the igniter fuel by electrical heating. Ignition is easily detectable by viewing smoke out of the exhaust nozzle.

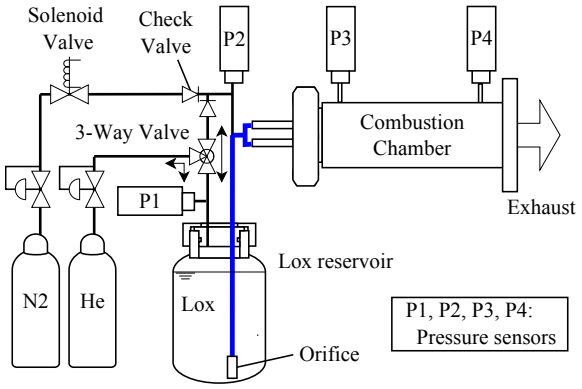

Fig. 3: Experimental apparatus.

A few seconds after ignition, the 3-way valve opens the line for applying pressure to the LOX reservoir and closes the GOX line simultaneously to start feeding LOX into the combustion chamber. After a prescribed firing duration, a valve relieves the pressure of the LOX reservoir to stop the feeding. Simultaneously, nitrogen gas purges the combustion chamber to stop firing quickly. Main measurement items during a firing were combustion chamber pressure and LOX flow rate. A differential pressure type flow meter in the LOX reservoir measures LOX flow rate. For test firings of Motor-A, a load cell measures axial thrust. After each firing test, residual fuel grain was recovered from the combustion chamber to measure the fuel consumption.

IV. RESULTS AND DISCUSSION

Errors due to the constant c^* assumption

To examine errors of RT-1 due to the constant c^* assumption, we compared results of RT-1 with those of RT-2. As mentioned above, RT-2 does not assume a constant c^*. Adopting RT-1 and RT-2, we obtained ξ histories in static firing tests with Motor-A. Table 2 summarizes test conditions of Motor-A firings. As might be expected, error due to the constant c^* assumption is small when ξ shift during firing is small. Test-3 is in such case, as Fig. 4 shows. In contrast, the error increases with

* Average value during a firing test.

Test index	LOX flow rate* [kg/s]	Initial fuel weight [kg]	Final fuel weight [kg]	Fuel consump -tion [kg]	Chamber pressure* [MPa]	Burning duration [s]	ω_ξ	ε_{12}	ω_η	ε_{23}	λ_1	λ_2	ε_{34}
1	1.76	25.6	17.2	8.4	1.96	10.2	0.105	0.074	0.022	0.040	0.79	0.77	0.01
2	2.73	25.4	18.6	6.8	3.30	5.5	0.116	0.060	0.031	0.078	0.88	0.87	0.00
3	1.30	25.4	20.4	5.0	1.30	6.9	0.054	0.019	0.023	0.074	0.79	0.76	0.01
4	1.84	25.4	20.5	4.9	2.22	5.3	0.068	0.029	0.017	0.027	0.84	0.83	0.00
5	2.24	25.4	20.4	5.0	2.72	4.8	0.099	0.035	0.018	0.035	0.71	0.69	0.01
6	2.09	25.4	20.7	4.7	2.18	5.0	0.043	0.026	0.018	0.039	0.72	0.71	0.00
7	2.59	25.3	20.3	5.0	2.58	4.9	0.059	0.038	0.023	0.053	0.78	0.77	0.00

Table 2: Test conditions and results of Motor-A firings.

a larger ξ shift, as Fig. 5 for Test-1 shows. To clarify the effect of ξ shift on the error due to the constant c^* assumption, we examined the effect of fluctuation range of ξ on mean relative error between RT-1 and RT-2. The following equations give a fluctuation range of ξ (=ω_ξ) and a mean relative error between RT-i and RT-j (=ε_{ij} i=1 and j=2 in this case), respectively, for each firing test;

$$\omega_\xi = \frac{1}{\overline{\xi}} \frac{\int_0^{t_b} \left| \overline{\xi} - \xi \right| dt}{t_b} \quad \text{where} \quad \overline{\xi} = \frac{M_o}{M_f} \tag{11}$$

$$\varepsilon_{ij} = \frac{1}{\overline{\xi}} \frac{\int_0^{t_b} \left| \xi_i - \xi_j \right| dt}{t_b} \tag{12}$$

Figure 6 shows the relationship between ω_ξ and ε_{12}; it clearly shows that ε_{12} increases with the increase in ω_ξ. The error due to the constant c^* assumption can be around 6% by a ξ fluctuation of 10%.

Errors due to the constant c^* efficiency assumption

RT-2 assumes a constant c^* efficiency. RT-3 avoids this assumption by using thrust history as additional input data. Accordingly, one can examine the error due to the constant c^* efficiency assumption by comparing results of RT-2 and RT-3 for each firing test. The following equation gives a fluctuation range of c^* efficiency (= ω_η) for each firing test;

$$\omega_\eta = \frac{\int_0^{t_b} \left| \overline{\eta} - \eta \right| dt}{t_b} \tag{13}$$

As Fig. 7 clearly shows, ε_{23} increases with the increase in ω_η. Although the c^* efficiency does not change unless the flow field structure greatly changes[8], it still requires attention because only 3% of c^* efficiency fluctuation can cause up to 8% error due to the constant c^* efficiency assumption.

Choice of nozzle discharge coefficient or thrust deduction coefficient

RT-3 and RT-4 assumes a constant nozzle discharge coefficient (=λ_1) and a constant thrust deduction coefficient (=λ_2), respectively. Because the momentum thrust (the first term of the right-hand side of equations (9) and (10)) accounts for most of the thrust, the two methods give close agreement with each other, as Fig. 8 shows. The physical background of λ_1 is that it accounts for non-isentropicity of the flow; it tends to reduce both

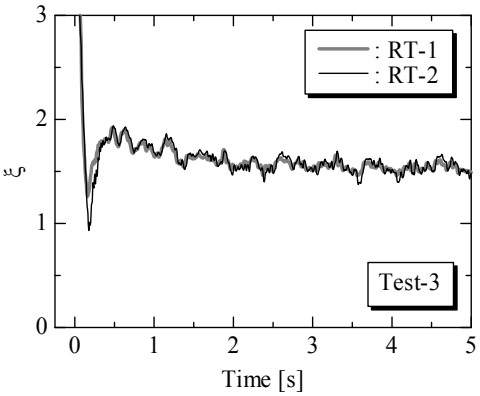

Fig. 4: ξ histories of Test-3.

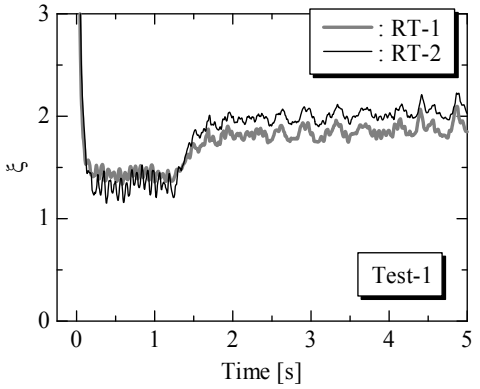

Fig. 5: ξ histories of Test-1.

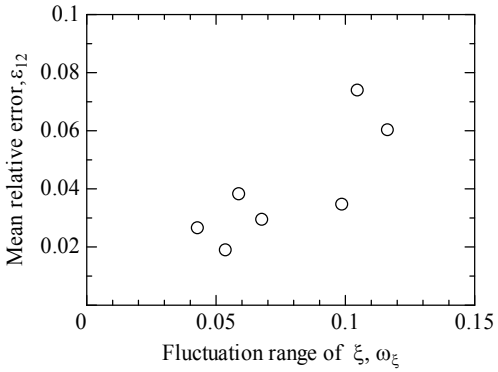

Fig. 6: Relationship between fluctuation range of ξ and mean relative error between RT-1 and RT-2.

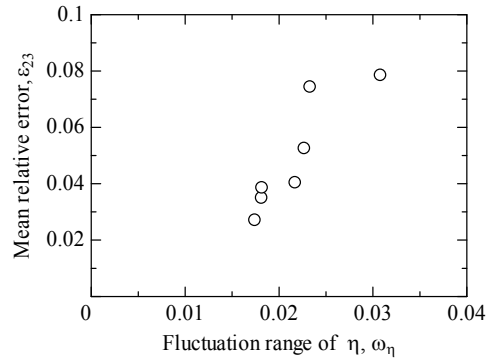

Fig. 7: Relationship between fluctuation range of η and mean relative error between RT-2 and RT-3.

* Average value during a firing test.
** Initial fuel weight is 683 g.

Test index	LOX flow rate* [g/s]	Final fuel weight [g]	Fuel consump -tion** [g]	Chamber pressure* [MPa]	Burning duration [s]
1	52	245	438	0.94	10.5
2	35	323	360	0.63	9.8

Table 3 Test conditions of Motor-B firings.

the actual mass flow rate and exit velocity comparing with the ideal case[8]. If the non-isentropicity of the flow has the same effect on the pressure thrust (the second term of the right-hand side of equations (9) and (10)), one can understand the physical meaning of λ_2 in the same manner. Unfortunately, it does not always hold; because the non-isentropicity of the flow tends to increase the nozzle exit pressure, the absolute value of the pressure thrust also increases when it is in an under-expansion condition. Accordingly, from a physical point of view, RT-3 is more appropriate than RT-4.

Overcoming multiple solution problem

Because RT-2, RT-3, and RT-4 include solving Eq. (6), we encounter a difficulty when Eq. (6) has multiple solution. To clarify the range of ξ in which this difficulty occurs, we rearrange Eq. (6) as follows:

$$\eta c^*_{th}(\xi,\, p_c)\left(1+\frac{1}{\xi}\right)=\frac{p_c A_t}{\dot{m}_o} \qquad (14)$$

Figure 9 shows the left hand side of Eq. (9) for polyethylene, PMMA, and polystyrene, together with the theoretical c^*, when the c^* efficiency η is unity. In these three fuels, only PMMA has the multiple solution problem. Figure 10 shows an enlarged view for PMMA. In a ξ range of 0.6 to 1.0, this function has multiple ξ to give a single output value.

We adopted RT-1 to static firing tests of Motor-B, which employs PMMA as a solid fuel. Table 3 shows test conditions. Figure 11 shows histories of chamber pressure and calculated ξ obtained for the test-2, showing an example encountering this difficulty. Mean flow rates of LOX and fuel were 35 g/s and 36.7 g/s, respectively. The mean ξ of 0.95 is in the multiple solution range. As a result, the ξ history shows a large fluctuation ranging from 0.6 to 0.9 during 3.5 s to 6 s. By employing RT-5, we can overcome this difficulty. Figure 12 shows results of RT-2 and RT-5 for Test-2; the fluctuation during 3.5 s to 6 s in RT-2 diminishes in RT-5.

Although RT-5 can overcome the multiple solution problem, it can cause an error due to the use of ξ obtained by RT-1 for the left-hand side of Eq. (6). Because RT-1

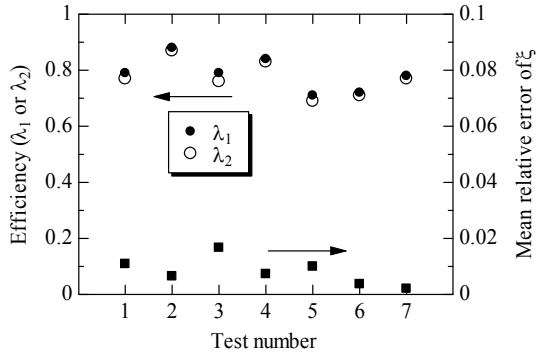

Fig. 8: Discharge coefficient, thrust deduction coefficient, and mean relative errors between RT-3 and RT-4 for each firing test.

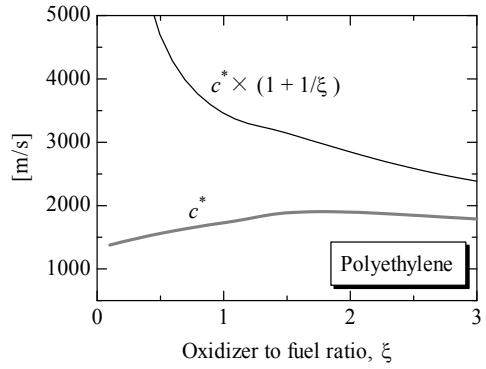

(*a*) Polyethylene

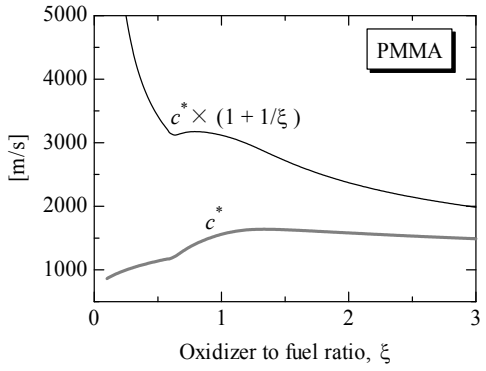

(*b*) PMMA

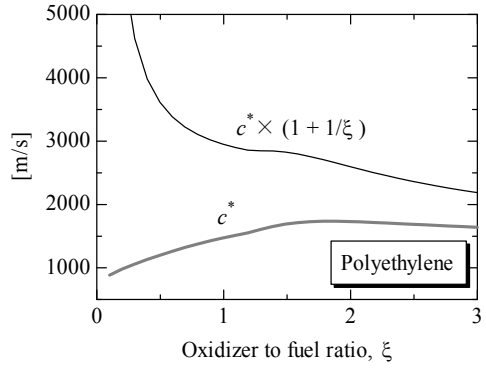

(*c*) Polyethylene

Fig. 9: Variations of c^* (theoretical) and $c^*\left(1+\frac{1}{\xi}\right)$ depending on ξ. The chamber pressure is 1 MPa.

can also avoid the problem, RT-5 is useful only when the result of RT-5 is more accurate than RT-1. The following equation gives the solution by RT-5 (= ξ_5);

$$\eta c_{th}^{*}\left(1+\frac{1}{\xi_5}\right)=\frac{p_c A_t}{\dot{m}_o}\equiv R \Leftrightarrow \xi_5=\frac{\eta c_{th}^{*}}{R-\eta c_{th}^{*}} \qquad (15)$$

By differentiating both sides with respect to c^*_{th},

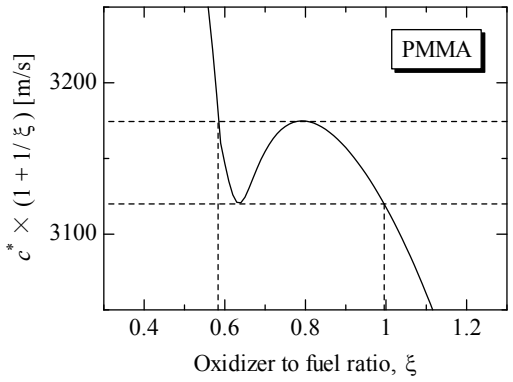

Fig. 10: Variation of $c^*\left(1+\frac{1}{\xi}\right)$ as a function of ξ around the range of multiple solutions.

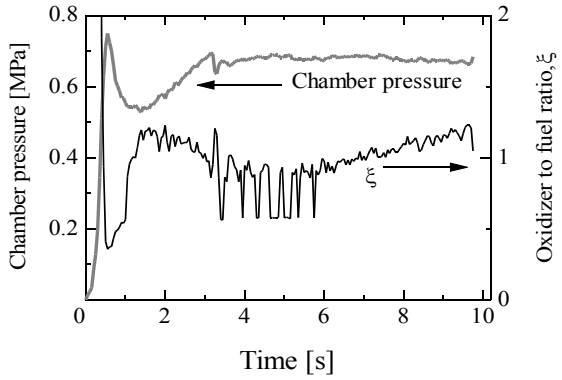

Fig. 11: A fluctuating ξ history as an example encountering the difficulty of multiple solutions.

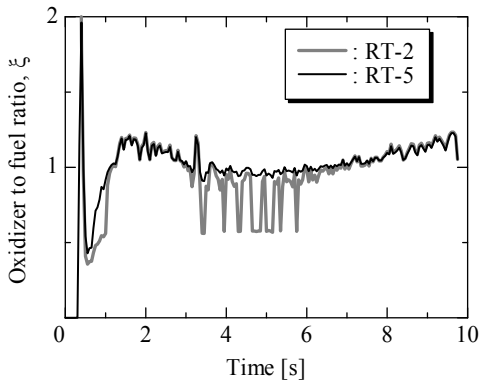

Fig. 12: ξ histories obtained by RT-2 and RT-3.

$$\frac{\partial \xi_5}{\partial c_{th}^{*}}=\frac{\eta\left(R-\eta c_{th}^{*}\right)+\eta^2 c_{th}^{*}}{\left(R-\eta c_{th}^{*}\right)^2}=\frac{\eta^2 R}{\left(R-\eta c_{th}^{*}\right)^2} \qquad (16)$$

Because RT-2 gives the exact solution (= ξ_2), the errors for RT-1 and RT-5 are given by

$$\delta_1=\xi_1-\xi_2, \quad \delta_5=\xi_5-\xi_2. \qquad (17)$$

Assuming that ξ_1, ξ_2, and ξ_5 are close in value to one another, we can approximate the ratio of δ_1 to δ_5 as

$$\frac{\delta_5}{\delta_1}\cong\frac{\partial \xi_5}{\partial \xi_1}=\frac{\partial \xi_5}{\partial c_{th}^{*}}\frac{\partial c_{th}^{*}}{\partial \xi_1}=\frac{\eta^2 R}{\left(R-\eta c_{th}^{*}\right)^2}\frac{\partial c_{th}^{*}}{\partial \xi_1} \qquad (18)$$

By substituting Eq. (15) into Eq. (18) to eliminate R,

$$\frac{\delta_5}{\delta_1}\cong\frac{\xi_5\left(\xi_5+1\right)}{c_{th}^{*}}\frac{\partial c_{th}^{*}}{\partial \xi_1} \qquad (19)$$

Again, by assuming that ξ_1 and ξ_5 are close in value with each other and ξ stands for the both,

$$\frac{\delta_5}{\delta_1}\cong\frac{\xi\left(\xi+1\right)}{c_{th}^{*}}\frac{\partial c_{th}^{*}}{\partial \xi} \qquad (20)$$

Figure 13 shows Eq. (20), the left-hand side in the vertical axis and ξ in the horizontal axis. In most of the normal operating ξ range, δ_5 is less than δ_1. Especially around the optimal ξ (around 1.35), δ_5 is much smaller than δ_1.

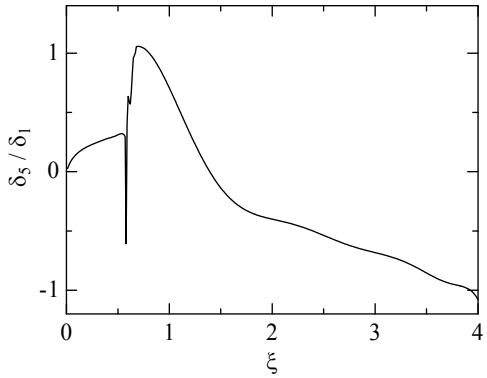

Fig. 13: Variation of δ_5/δ_1 as a function of ξ (Eq. (20)).

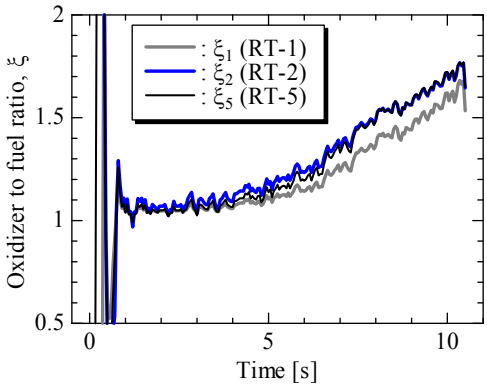

Fig. 14: ξ histories obtained by RT-1, RT-2, and RT-5.

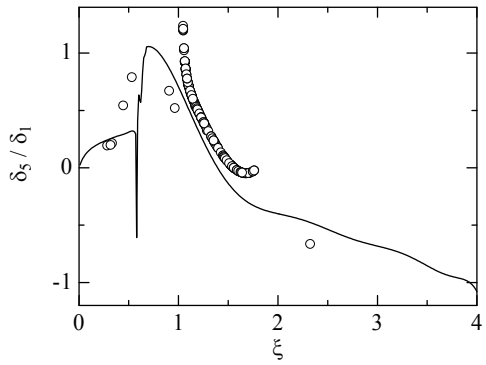

Fig. 15: Temporal relationships between δ_5/δ_1 and ξ for Test-1 (open circles), together with the approximate relationship.

When ξ stays out of the multiple solution range during a firing test, the multiple solution problem does not arise. Test-1 belongs to this case. Figure 14 shows ξ histories obtained by RT-1, RT-2, and RT-3. Over the entire burning period, ξ_5 is closer to ξ_2 than ξ_1 to ξ_2. In the latter half of the period, ξ_5 gives close agreement with ξ_2. Figure 15 shows temporal relationships between δ_5/δ_1 and ξ for Test-1, together with the approximate relationship Fig. 13 shows. The temporal plots (open circles) are close to the line giving the approximate relationship, showing that the approximation is reasonable. Although δ_5 is comparable to δ_1 in the range of multiple solution problem (of ξ from 0.6 to 1.0), δ_5 is still less than δ_1. Accordingly, RT-5 can overcome the multiple solution problem and gives ξ more accurately than RT-1.

V. CONCLUSION

Accuracies and applicable ranges of five data reduction methods, RT-1 to RT-5, were evaluated experimentally. RT-1 determines the fuel consumption rate as a function of time from histories of the chamber pressure and the oxidizer flow rate, assuming a constant c^* during firing. Three of other methods obtain O/F (=ξ) by solving an equation between theoretical and experimental c^* values without assuming a constant c^*. RT-2 uses histories of chamber pressure and oxidizer flow rate, assuming a constant c^* efficiency. The third and fourth one (RT-3 and RT-4) eliminates the need for the assumption of a constant c^* efficiency by employing thrust history as additional input data. The difference between the two methods is that RT-3 assumes a constant nozzle discharge coefficient whereas RT-4 assumes a constant thrust efficiency. From RT-2 to RT-4, a difficulty arises when multiple solutions of ξ exists in the equation between theoretical and experimental c^* values. RT-5 avoids this difficulty by merging two methods: RT-1 and RT-2.

Because the c^* variation due to the ξ shift during a firing is not an uncommon feature in hybrid rockets, the constant c^* assumption can cause error. The error in ξ increases with increasing the fluctuation range of ξ in a firing test. Experimental results show that ξ fluctuation of 10% can cause errors of around 6% in ξ. RT-2 can cause error due to the constant c^* efficiency assumption. Although the c^* efficiency does not change unless the flow field structure greatly changes, it still requires attention because only 3% of c^* efficiency fluctuation can cause up to 8% error in ξ.

RT-5 can cause an error due to the use of ξ obtained by RT-1 for the function giving theoretical c^*. Although the error of RT-5 (=δ_5) is comparable to the error of RT-1 (=δ_1) in a certain ξ range, δ_5 is still less than δ_1. Accordingly, RT-5 can overcome the multiple solution problem and gives ξ more accurately than RT-1.

ACKNOWLEDGEMENT

This research is supported by the Ministry of Education, Science, Sports and Culture, Grant-in-Aid for Scientific Research (A), 40281787, 2012.

This research is supported by the Hybrid Rocket Research Working Group (HRrWG) of Institute of Space and Astronautical Science, Japan Aerospace Exploration Agency. The authors thank members of HRrWG for their helpful discussion.

REFERENCES

[1] Frederick Jr., R. A. and Greiner, B. E., *Journal of Propulsion and Power*, **12**(3), 605-611, 1996.

[2] Karabeyoglu, M. A., Cantwell, B. J. and Zilliac, G., *Journal of Propulsion and Power*, **23**(4), 737-747, 2007.

[3] Osmon, R. V., *Aerospace Chemical Engineering*, 62(61), 92-102, 1966.

[4] Nagata, H., Nakayama, H., Watanabe, M., Wakita, M, and Totani, T., *Advances in Aircraft and Spacecraft Science*, Vol. 1, No. 3, 273-289, 2014.

[5] George, P., Krishnan, S., Varkey, P. M., Ravindran, M. and Ramachandran, L., *Journal of Propulsion and Power*, 17(1), 35-42, 2001.

[6] Nagata, H., Ito, M., Maeda, T., Watanabe, M., Uematsu, T., Totani, T. and Kudo, I., *Acta Astronautica*, **59**(1-5), 253-258, 2006.

[7] Wernimont, E.J. and Heister, S.D., *Journal of Propulsion and Power*, **15**(1), 128-136, 1999.

[8] Carmicino, C and Sorge, A. R., *Journal of Propulsion and Power*, **22**(5), 984-995, 2006.

[9] Gordon, S. and McBride, B. J., *NASA Reference Publication*, RP-1311, 1994.